International Conference on Mathematics, Computational Methods & Reactor Physics (M&C 2009)
Saratoga Springs, New York, May 3-7, 2009, on CD-ROM, American Nuclear Society, LaGrange Park, IL (2009)

DEVELOPMENT AND PERFORMANCE OF THE ANDES/COBRA-III COUPLED SYSTEM IN HEXAGONAL-Z GEOMETRY

J. A. Lozano*, J. Jimenez, N. García-Herranz and J.M. Aragonés
Department of Nuclear Engineering
Universidad Politécnica de Madrid, c/ José G. Abascal 2, 28006 Madrid, Spain
lozano@din.upm.es; jimenez@din.upm.es; nuria@din.upm.es; arago@din.upm.es

ABSTRACT

In this paper, the extension of the nodal diffusion code ANDES, based on the ACMFD method, to hexagonal geometry is presented, as well as its coupling with the thermal-hydraulic (TH) code COBRA-IIIc/MIT-2 for such hexagonal problems.

In extending the ACMFD method to hexagonal assemblies, triangular-Z nodes are used, taking advantage of the mesh refinement capabilities implicit within that geometry.

The existing TH coupling for Cartesian geometry applications has also been extended to hexagonal problems, with the capability to model the core using either assembly wise channels (hexagonal mesh) or a higher refinement with six channels per fuel assembly (triangular mesh). Achieving this level of TH mesh refinement with COBRA-IIIc code provides a better estimation of the in-core 3D flow distribution. Therefore, the work presented here introduces an improvement in the TH VVER core modelling, where in the best case scenario, just twenty axial layers and one channel per fuel assembly were used.

As a result, the neutronic and thermal-hydraulics (N-TH) coupled code, ANDES/COBRA-IIIc, extensively verified in Cartesian geometry cores analysis, can also be applied to full three-dimensional VVER core problems. Some verification results are provided, corresponding to 2nd exercises (HZP and HP steady states) of the OECD/NEA- VVER-1000 Coolant Transient benchmark and to the HZP and HFP steady states of the V1000CT2-EXT2 NURESIM benchmark.

Key Words: ANDES, neutronic-thermalhydraulics coupling, hexagonal geometry, coarse mesh scale.

1. INTRODUCTION

During the last years, the reactor physics group at UPM has been working in the development of the in-house neutron diffusion code *ANDES* based on the ACMFD method developed by Y.A. Chao in 1999 [1]. This methodology was extended to 3D Cartesian geometry and multigroups [2] and implemented in the *ANDES* code [3], [4] for LWR analysis, showing a very good numerical performance in terms of mesh refinement and computing time. *ANDES* was also coupled with the thermal-hydraulic (TH) code *COBRA-IIIc/MIT-2* [5] allowing analysis of LWR at coarse mesh scale for both HP steady state and transient calculations [6], [7].

* Corresponding author
Tel: +34 91 336 3108; Fax: +34 91 336 3102

In this paper, we address the extension of the ACMFD method to triangular-Z geometry and its application to reactor cores with hexagonal fuel assemblies (VVER, HTGR, SFR). There are several reasons to use triangular nodes: first, it allows to refine the mesh any number of times and, second, it allows to have a better modelization of the TH and burn-up effects. The details of the formulation, paying special attention to the transverse integration of the diffusion equation in triangular geometry will be summarized in Section 2.

The existing TH coupling has also been extended to hexagonal geometry with the capability to model the core using either assembly wise channels (hexagonal mesh) or a higher refinement with six channels per fuel assembly (triangular mesh). The new coupling scheme and its peculiarities will be explained in Section 3.

As a result of the research efforts explained above, a new best-estimate code for VVER core analyses has been developed. In Section 4, we verify the performance of *ANDES/COBRA-IIIc* coupled system with the steady state cases specified in the V1000CT2-EXT2 Benchmark [8] and the exercise 2 of the OECD/NEA VVER-1000 Coolant Transient Benchmark [9]. The results corresponding to the transient calculation are provided and the influence of the mesh refinement is analyzed.

2. THE ANALYTIC COARSE MESH FINITE DIFFERENCE METHOD IN TRIANGULAR-Z GEOMETRY

The ACMFD method in Cartesian geometry [2] is based on two steps aimed to obtain an analytical intranodal flux shape which determines the nodal coupling equation. The first one is the decoupling of the multigroup diffusion equation by means of diagonalization of the multigroup diffusion matrix. This way we obtain a set of uncoupled diffusion equations over the modal fluxes which are linearly related to the physical fluxes. The second procedure is applied only in multidimensional applications to overcome the problems derived from a non-closed analytic solution of the diffusion equation. In those cases, a transverse integration is performed and thus, the n-dimensional diffusion equation is transformed into n 1-D diffusion equations over the 1-D averaged flux. These equations are coupled through the external source term which includes the transverse leakage.

In this paper, we demonstrate that the extension of the ACMFD method to triangular-Z geometry does not involve a substantial change in this procedure. The hexagonal assemblies are divided into six triangular right prisms, composed of five interfaces (two equilateral triangular bases and three rectangular sides).

As explained previously, the first step to obtain the ACMFD relation at each nodal interface is the decoupling of the multigroup diffusion equation; this procedure is independent on the geometry. However the second step, that is, the transverse integration process to reduce the 3D diffusion equation to three 1-D diffusion equations, requires additional developments. For triangular geometry, we will show that expressions are much more complex and further manipulation of the equations is needed.

2.1. Transverse Integration of the 3D Diffusion Equation in Triangular Prismatic Nodes

Let us start from the 3D neutron diffusion modal equation within our homogeneous triangular-prismatic nodal volume V shown in Figure 1:

$$-\nabla \cdot \vec{j}_m(\vec{r}) - \lambda_m \psi_m(\vec{r}) = -s_m(\vec{r}) \;\; ; \;\; \vec{j}_m(\vec{r}) = -\nabla \psi_m(\vec{r}) \quad \text{m=1,}\cdots\text{,G} \tag{1}$$

where λ_m is the modal eigenvalue, $s_m(r)$ the modal external source and G the number of energy groups.

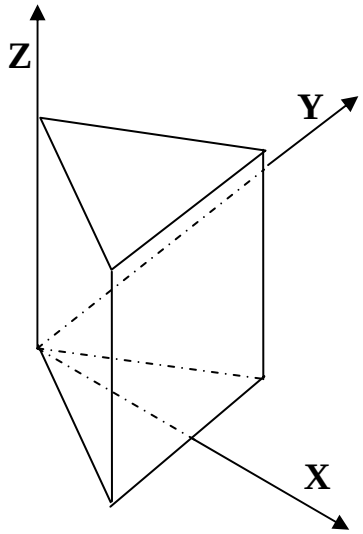

Figure 1. Node in triangular-Z geometry.

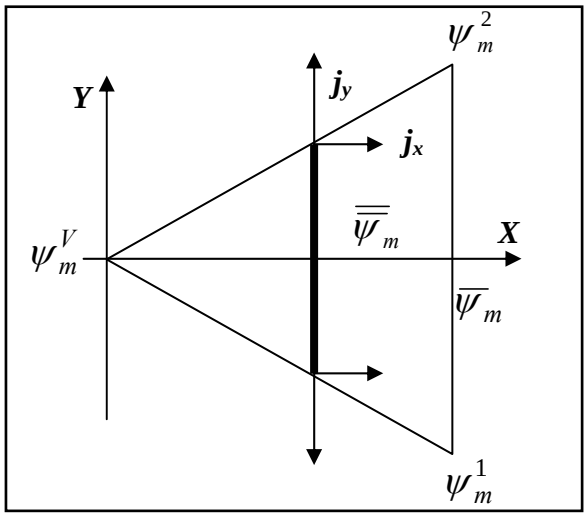

Figure 2. Components of the modal current in the XY plane and magnitudes involved in the ACMFD relation.

The transverse integration procedure in the axial direction (Z) is used to obtain the ACMFD relation at the top and bottom interfaces of the node, in the same way as in Cartesian geometry. However, let us see the form of the resulting equations when applying the transverse integration approach in the radial directions (X or Y).

Let us consider the transverse integration over the X direction. Integrating equation (1) over a slice of width dx perpendicular to the X axis, we obtain the following equation over the flux integrated in the slice:

$$\frac{d^2\psi_m^{1D}(x)}{dx^2} - \lambda_m \psi_m^{1D}(x) = -s_m^{1D}(x) + L_m(x) \tag{2}$$

$$\begin{aligned} \psi_m^{1D}(x) &= \int_0^{H_Z} \left[\int_{-ax}^{ax} \psi_m(x,y,z) \cdot dy \right] \cdot dz \;\; ; \;\; a = \frac{1}{\sqrt{3}} \\ s_m^{1D}(x) &= \int_0^{H_Z} \left[\int_{-ax}^{ax} s_m(x,y,z) \cdot dy \right] \cdot dz \end{aligned} \tag{3}$$

$L_m(x)$ is a term equivalent to the transverse leakage in Cartesian nodes, although in this case it has a major complexity:

$$\begin{aligned} L_m(x) = &-\frac{2}{\sqrt{3}}\int_0^{H_Z}\left(j_{m,x}(x,\frac{x}{\sqrt{3}},z) + j_{m,x}(x,-\frac{x}{\sqrt{3}},z)\right)\cdot dz + \\ &+\frac{2}{3}\int_0^{H_Z}\left(j_{m,y}(x,\frac{x}{\sqrt{3}},z) - j_{m,y}(x,-\frac{x}{\sqrt{3}},z)\right)\cdot dz + \\ &+\int_{-ax}^{ax}\left(j_{m,z}(x,y,H_Z) - j_{m,z}(x,y,0)\right)\cdot dy \end{aligned} \qquad (4)$$

where $j_{m,x}$, $j_{m,y}$ and $j_{m,z}$ are the components of the vectorial current in the modal space (see Figure 2). For example, $j_{m,x}(x,y,z) = -\dfrac{\partial \psi_m(x,y,z)}{\partial x}$.

As it can be seen, as occurs in Cartesian geometry nodes, the transverse integrated flux is the unknown of the resulting 1D diffusion equation obtained after integration of the original 3D equation along a radial direction. It is important to clarify that, now, the radial transverse leakage does not fit the net leakage through the side faces of the prism. However, we will maintain its name as it plays the same role as in the case of Cartesian geometry.

Following, it will be shown how the ACMFD relation at a radial interface in triangular-Z geometry can be derived, that is, how to relate both node surface currents and fluxes to node average fluxes.

2.2. The ACMFD Relation at Radial Interfaces in 2D Triangular Nodes

For simplicity, we will consider first the 2-D geometry case, that is, the triangular node shown in Figure 2. As it can be seen in equation (2), the transverse integrated flux being solution of a 1D diffusion equation can be expressed by the following analytic functions:

$$\psi_m^{1D}(x) \;=\; A_m\, e^{+\alpha_m x} \;+\; B_m\, e^{-\alpha_m x} \;+\; p_m(x)\;;\; \frac{d^2}{dx^2}p_m(x) \;-\; \lambda_m\, p_m(x) = L_m(x)\;;\; \alpha_m = \sqrt{\lambda_m} \qquad (5)$$

A_m and B_m are constants that can be determined by imposing the following conditions: the modal interface average flux at a radial interface $\bar{\psi}_m$, the modal average current at the same interface $\bar{j}_m$ and the modal fluxes at the corners adjacent to the interface ψ_m^1 and ψ_m^2. Then, substituting in the node-average modal flux $\bar{\bar{\psi}}_m$, the ACMFD modal relation at every radial interface in triangular mesh is obtained:

$$\left(\bar{\psi}_m - \frac{p_m(\frac{\sqrt{3}}{2}L)}{L} \right) = \frac{C_m^f}{2}\left(\bar{\bar{\psi}}_m - \frac{2\bar{p}_m}{L} \right) + \frac{C_m^j}{4}\left(\psi_m^1 + \psi_m^2 \right) - \frac{\sqrt{3}}{4} L C_m^j \left(\bar{j}_m + \frac{p'_m(\frac{\sqrt{3}}{2}L)}{L} \right) \qquad (6)$$

where L is the triangle side length and C_m^f and C_m^j are the analytic coefficients defined in [2].

Attending to expression (6), and comparing it with the equivalent relation in Cartesian geometry, we can see that the main drawback is the presence of the modal fluxes at the two corners adjacent to the interface, which have to be computed with a level of accuracy appropriate to this high order method.

2.3. The Analytic Relation at Corners in 2D Triangular Nodes

To obtain the modal flux at a corner, we proceed as follows. We can particularize expression (5) at the coordinate ($x = 0$), which corresponds to the triangle vertex opposed to the analyzed interface. If we focus on the values of the function and its first derivative at this coordinate, then we will obtain the following relation between the flux at vertex and the nodal average flux results:

$$\left(\psi_m^V - \frac{\sqrt{3}\cdot p'_m(0)}{2} \right) = D_m^f \left(\bar{\bar{\psi}}_m - \frac{2\cdot\bar{p}_m}{L} \right) + D_m^j \frac{p_m(0)}{L}$$
$$D_m^f = \frac{\gamma^2}{e^{\gamma} + e^{-\gamma} - 2} \quad ; \quad D_m^j = \frac{\gamma\cdot\left(e^{\gamma} - e^{-\gamma}\right)}{e^{\gamma} + e^{-\gamma} - 2} \quad ; \quad \gamma = \frac{\sqrt{3}}{2}\alpha_m L \qquad (7)$$

2.4. Combination of the ACMFD Relation at a Radial Interface with the Analytic Relations at the Adjacent Corners

Until now, it has been demonstrated that, as occurs in Cartesian geometry nodes, it also exists an ACMFD relation for triangular nodes. Nevertheless, we have also found that the flux particularized at adjacent vertexes takes part in such ACMFD relation. In order to obtain a linear system in which nodal average fluxes are the unique unknowns, an additional relation between the flux at a vertex and the nodal average flux has been derived.

The most straightforward option to treat equation (6) would be to take the term of fluxes at vertex from the previous iteration, including them in the non-linear iteration loop (as done with the transverse leakage term). However, this option is unfeasible as the iterative process becomes unstable because of the excessive influence of the transverse leakage term.

Consequently, it is necessary to substitute the flux at vertexes in relation (6) by their corresponding relation with the nodal average flux (7). Computing and grouping together the transverse leakage terms, we obtain the following expression:

$$\bar{\psi}_m = C_m^f \bar{\bar{\psi}}_m - \frac{\sqrt{3}}{4} L C_m^j \bar{j}_m - T_m^{S*} \tag{8}$$

This way we finally have an expression quite similar to the ACMFD for Cartesian nodes, but in this case the transverse leakage profile has less physical meaning than in the previous one.

However, this methodology will not lead to the level of accuracy achieved with Cartesian geometry. The reason of this assertion is that the accuracy of the analytic nodal method relies on a good estimation of the average value of the transverse leakage. In Cartesian mesh this average value only depends on the interface average currents whose error vary from 0.1% to 1% in most of nodal solutions. Nevertheless attending to the transverse leakage expression in triangular mesh (4) we can see that transverse leakage not only gather the perpendicular component of current to the surface, but also the tangential one. This will force us to compute the flux at the three vertexes of every node.

2.5. Extension of ACMFD Theory to 3D (Triangular-Z Geometry)

In triangular-Z geometry, the main difficulties arise from the fact that the transverse area changes in the radial direction. Once provided the formulation for 2D triangular nodes, the extension to the 3D case is not difficult. We will have to overcome two additional aspects. First, an ACMFD relation for axial top and bottom interfaces has to be derived. Second, the transverse leakage has to be redefined to include the axial component as well, that is, the neutron leakage through the top and bottom interfaces has to be taken into account in the particular solution of equation (6), then the transverse leakage $L_m(x)$ is modified.

2.5.1. The ACMFD relation for axial interfaces

As it has been explained in previous sections, the first step to obtain an ACMFD relation is to perform a transverse integration of the 3D diffusion equation. In this case the integration is over the triangular area perpendicular to the Z axis. In axial direction, the transverse area is constant, so the procedure to obtain the ACMFD relation is the same as in Cartesian nodes. Starting from the 3D modal equations we obtain the 1D modal equation over the 1D averaged flux:

$$\begin{aligned} &\frac{d^2\psi_m^{1D}(z)}{dz^2} - \lambda_m \psi_m^{1D}(z) = -s_m^{1D}(z) + L_m(z) \\ &L_m(z) = \frac{4}{\sqrt{3}L} \sum_{r=1}^{3} j_{m,r}(z) \end{aligned} \tag{9}$$

where $j_{m,r}(z)$ is the averaged outgoing current through radial interfaces at height z.

Independently the way we obtain the transverse leakage $L_m(z)$, equation (9) leads to an ACMFD relation similar to the Cartesian one with the only particularity that the transverse leakage is computed in a different way.

2.5.2. Modifications of the ACMFD relation for radial interfaces in 3D nodes

In 3D nodes, equation (4) can be written in the following way:

$$L_m(x) = L_m^R(x) + \int_{-ax}^{ax} \left(j_{m,z}(x,y,H_Z) - j_{m,z}(x,y,0) \right) \cdot dy = L_m^R(x) + L_m^Z(x) \tag{10}$$

The transverse leakage profile in Z-direction leads to an additional particular solution. Then equation (5) is modified:

$$\begin{aligned} \psi_m^{1D}(x) &= A_m \, \mathrm{e}^{+\alpha_m x} + B_m \, \mathrm{e}^{-\alpha_m x} + p_m^R(x) + p_m^Z(x) \\ \frac{d^2}{dx^2} p_m^Z(x) &- \lambda_m \, p_m^Z(x) = L_m^Z(x) \end{aligned} \tag{11}$$

Finally it is worthy to remark that if we want to assume a polynomial profile for $L_m^Z(x)$, we will have to take into account that the integration length in (10) varies with x.

3. THE N-TH COUPLING SCHEME FOR HEXAGONAL PROBLEMS

The N-TH coupling in *ANDES/COBRA-IIIc* was originally developed for 3D Cartesian geometry [7], [10], including the capability of refining the radial mesh by using both one or four neutronic nodes and one or four channels per fuel assembly. The use of the TH channel code *COBRA-IIIc* in LWR provides an accurate estimation of the in-core 3D flow distribution due to the treatment of cross flows between adjacent channels.

The next step in the coupling scheme development has been its extension to VVER cores by addressing the challenging hexagonal mesh geometry of this type of reactors. The objective is to maintain the capability of performing a radial mesh refinement, and to take advantage of the cross flow treatment to provide an accurate estimation of the 3D flows also in hexagonal geometry problem applications.

With this aim, the N-TH coupling extension to hexagonal geometry has been recently carried out. The coupled *ANDES/COBRA-IIIc* code has the capability to model the core using either assembly wise channels (hexagonal channels) or six channels (triangular channels) per fuel assembly if a higher level of refinement is required in the TH radial nodalization. Regarding the axial meshing, the only restriction to the node height is related to the stability of both N and TH solvers. The required stability imposes a number of axial nodes varying between a minimum value of ten axial layers up to forty, depending on the strength of the feedback in the axial direction.

In order to verify the adequacy of the coupled code, several exercises of the VVER-1000 Coolant Transient Benchmark [9] have been performed. In the TH core modelling of this benchmark, most of participants considered just twelve axial layers and several fuel assemblies were represented by a single homogenized 1D channel. The capability of the TH mesh refinement

with COBRA-IIIc code allows to improve the TH VVER core modelling, providing a better estimation of the in-core 3D flow distribution. This will be demonstrated in Section 4.

4. VERIFICATION RESULTS

The verification of the *ANDES/COBRA-IIIc* extension to hexagonal geometry has been carried out using the second exercise of the V1000CT2-EXT2 [8] and the second exercise of the V1000CT-1 Benchmark [9]. In order to model properly the fuel behaviour in the above exercises, a polynomial fitting for the fuel, gap and cladding properties (thermal conductivity and heat capacity) was developed from the benchmark specifications to take into account their dependence with temperature. Those polynomials were implemented as correlations within the code *COBRA-IIIc/MIT-2*.

Table I presents the results corresponding to different steady state situations proposed in the V1000CT2-EXT2 Benchmark [8]. The case "2" corresponds to a HFP condition, the others, are at HZP with different control rods positions. Two results are provided for each single case, one using six neutronic nodes per fuel assembly and another using twenty four neutronic nodes per fuel assembly.

Table I. *ANDES/COBRA-III* results for the V1000CT2-EXT2 steady state cases

Case		K_{eff}	F_{xy}	F_z	*A.O.* (%)
0	**6N***	1.03013	1.339	2.967	80.68
	24N**	1.03005	1.340	2.964	80.62
1a	**6N**	0.99688	1.427	1.716	41.98
	24N	0.99673	1.421	1.708	41.62
2	**6N**	0.99851	1.352	1.199	5.11
	24N	0.99845	1.350	1.199	5.15
3	**6N**	0.96895	6.564	2.116	56.96
	24N	0.96872	6.495	2.112	56.80
4	**6N**	0.96894	6.570	2.111	56.79
	24N	0.96871	6.500	2.108	56.64

*6N: 6 radial neutronic nodes per assembly, **24N: 24 radial neutronic nodes per assembly

From Table I, it can be figured out that the refinement in the radial direction does not change very much the radial peaking factor (F_{xy}). Besides, the differences in k_{eff} are lower than 23 pcm even in the cases "3" and "4" which are highly asymmetric due to the insertion of one control rod close to the periphery. This demonstrates the high order of our ACMFD method, since it is possible to obtain very accurate results using a coarse mesh for hexagonal geometry (just 6 triangular nodes per fuel assembly).

Next are presented the results obtained for the second exercise of the V1000CT-1 Benchmark [11]. The steady states at Hot Zero Power (HZP) and Hot Power (HP) are summarized in Table II

and Table III respectively. From here on, we will consider the average result of the benchmark participants, with its associated standard deviation, as the reference solution for our comparisons.

For the HZP steady state, our solution was obtained using ten axial layers within the active core plus two layers for the lower and upper axial reflectors. Furthermore six triangular nodes per fuel assembly were used for the neutronic radial nodalization. The results obtained for the HZP conditions show a very good agreement with the benchmark reference solution (they are within the standard deviation for all the parameters studied). Consequently, the extension of the nodal diffusion code *ANDES* to hexagonal geometry is demonstrated to be successful.

Table II. *ANDES/COBRA-III* result for HZP steady state in exercise 2

HZP case	K_{eff}	F_{xy}	F_z	*A.O.* (%)
REFERENCE RESULT	1.00022	1.416	1.519	16.88
(Standard deviation)	(±0.00083)	(±0.012)	(±0.007)	(±0.84)
ANDES/COBRA-III	0.99979	1.407	1.521	16.44
Deviation from the ref.	-0.00043	-0.009	+0.002	-0.44

Regarding the HP steady state, four different results (A, B, C, and D) are presented in Table III, changing the mesh refinement in both neutronic and thermalhydraulic sides. Result "A" was computed with the coarse mesh, using ten axial nodes, six triangular neutronic nodes and one hexagonal channel per fuel assembly. The results "B" and "C" had the same number of axial layers, twenty, and the same TH meshing, one hexagonal channel per fuel assembly, but they had different neutronic nodalizations. Result "B" was obtained using six triangular nodes per fuel assembly while result "C" used twenty four triangular nodes per fuel assembly. Finally, result "D" was calculated with the finest meshing, using forty axial layers, with triangular channels (six channels per fuel assembly) and six triangular neutronic nodes per fuel assembly.

Table III. *ANDES/COBRA-IIIc* results for HP steady state with several nodalizations

HP steady state	K_{eff}	F_{xy}	F_z	*A.O.* (%)
REFERENCE RESULT	0.99998	1.341	1.406	16.29
(Standard deviation)	(±0.00116)	(±0.011)	(±0.021)	(±1.28)
Result* A (6N/1TH/10Z)	1.00056	1.349	1.427	17.76
Deviation from the ref.	+0.00058	+0.008	+0.021	+1.47
***Result B* (6N/1TH/20Z)**	1.00061	1.349	1.431	18.23
Deviation from the ref.	+0.00063	+0.008	+0.025	+1.94
***Result C* (24N/1TH/20Z)**	1.00055	1.348	1.431	18.20
Deviation from the ref.	+0.00057	+0.007	+0.025	+1.91
***Result D* (6N/6TH/40Z)**	1.00053	1.347	1.433	18.44
Deviation from the ref.	+0.00055	+0.007	+0.027	+2.15

*(6N/1TH/10Z): 6 radial neutronic nodes, 1 thermal-hydraulics channel per fuel assembly, 10 axial layers

Looking at Table III, most of the discrepancies are in the axial power distribution, which is due to the different axial nodalization of the participants. Most of them just used twelve axial layers, which explains why the result "A" (with ten axial nodes) compares better against the reference solution in terms of Axial Offset (*A.O.*) and axial peaking factor (F_z). Those results show the strong dependence of the axial profile on the TH feedback.

Regarding the radial power distribution, a comparison of that magnitude extracted from the Result "B" (twenty axial layers and one channel per fuel assembly) against the reference solution in one sector of the core is presented in figure 3. It can be seen that *ANDES/COBRA-IIIc* distribution is in good agreement with the reference solution under the HP steady state condition (our deviation is within the standard deviation for almost all the nodes). Therefore, it is proved that the extension to hexagonal geometry of the coupling scheme has been properly implemented.

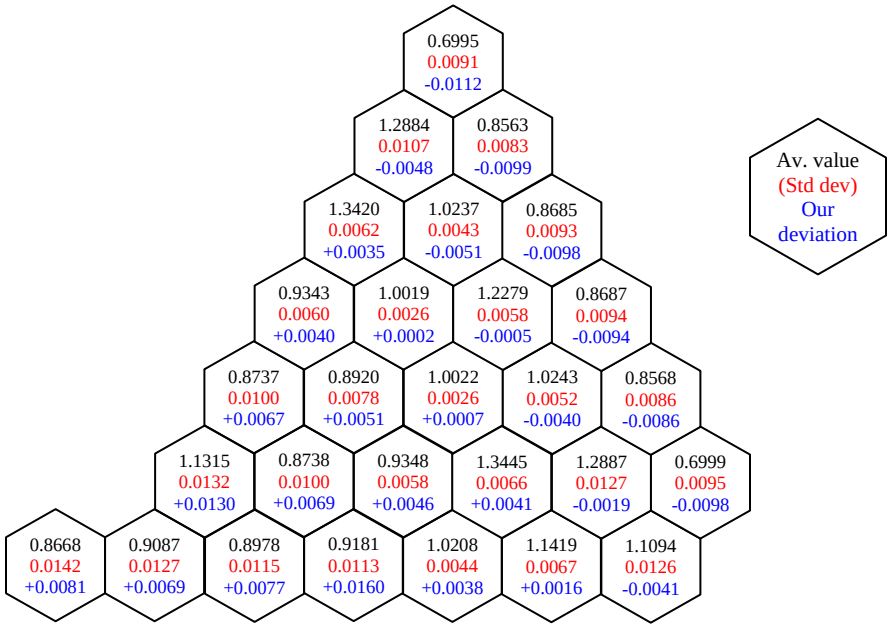

Figure 3. Radial power distribution comparison for the HP steady state.

After the steady state cases, we have run the guided transient using the boundary condition files provided with the benchmark documentation. In those files, the mass flow rate, coolant temperature and pressure conditions per fuel assembly versus time were specified. Because of the strong axial dependence of the TH feedback, in this exercise we used two different nodalizations: one using twenty axial layers and hexagonal channels, and other using forty axial layers and triangular channels. Both transient used the same neutronic nodalization (6 triangles per fuel assembly). The computed results are presented in figures 4, 5 and 6, where the mean values of the results obtained by the different participants in this transient exercise are also shown.

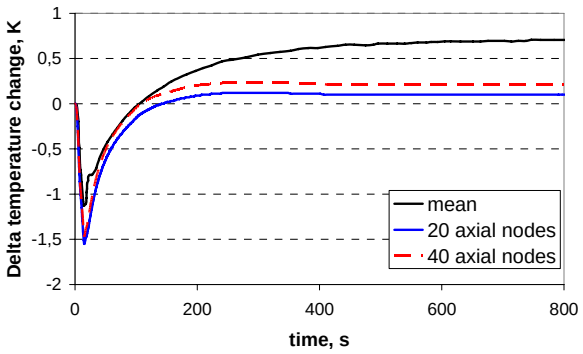

Figure 4. Time history of core average fuel temperature.

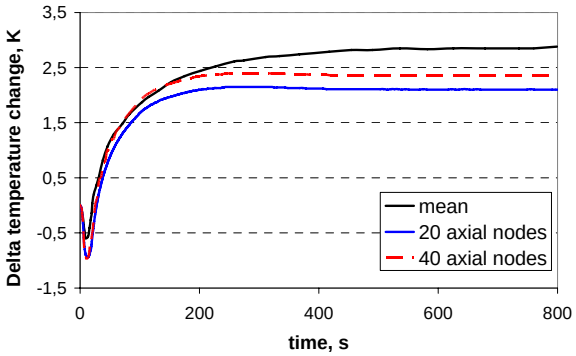

Figure 5. Time history of maximum nodal average fuel temperature.

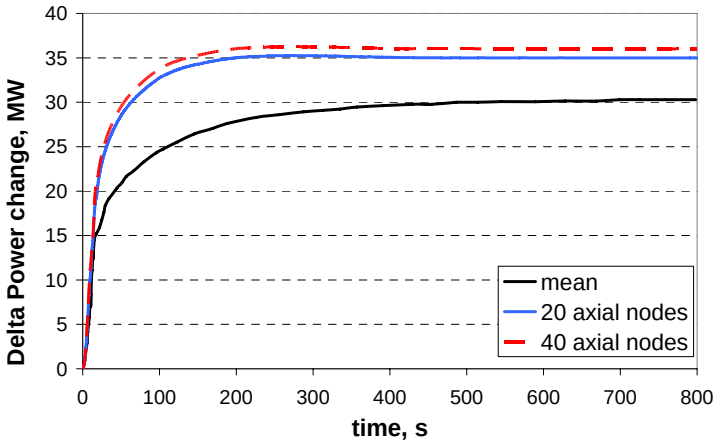

Figure 6. Time history of power

The deviations of the results with respect to the mean values could lead us to conclude that the performance in the transient calculation is not that good. However, if we take into account the wide spread of the results provided by the different participants, where the delta power change at 800 seconds varies from 21 to 45 MW, it could be said that the mean value can not be taken as a reference solution and that the coupled code *ANDES/COBRA-IIIc* reproduces accurately the transient scenarios

5. CONCLUSIONS

The coupled neutronics-thermalhydraulics ANDES/COBRA-IIIc code has been extended to hexagonal geometry applications.

As far as the neutronics, the extension of the ACMFD method has been carried out using triangular-Z nodes, taking advantage of the mesh refinement capabilities implicit when using this geometry instead of hexagonal nodes. The results obtained for the HZP cases show the high order of our ACMFD method, since it is possible to obtain very accurate results using a coarse

mesh for hexagonal geometry. The deviations in k_{eff} are lower than 20 pcm and the relative error in the assembly power is below 1%.

As far as the thermal-hydraulics, the coupling scheme has also been extended to hexagonal problems, with the capability to model the core using either hexagonal or triangular mesh. The use of COBRA-IIIc code with this level of TH mesh refinement provides an accurate estimation of the in-core 3D flow distribution.

The coupled code has been verified using an internationally well-known VVER benchmark. The results obtained for both steady-state and transient calculations have been used for verification purposes and have shown a quite good agreement with the reference solution. We have confirmed that *ANDES* has a good reliability for the kinetic calculations of reactor cores with hexagonal fuel assemblies, and we have proved that the extension of the coupling scheme has been properly implemented. Regarding the differences in the axial power distribution, we found that the results had a strong dependence on the fuel thermal solution, in particular, it was very sensitive to the implementation of the gap conductivity.

This verification of the coupled code system can be considered as a promising starting point for the development of a simulation tool for the proposed Gen IV advanced core designs using hexagonal fuel assembly configurations.

ACKNOWLEDGMENTS

This work is partially funded by the European Commission under the 6th EURATOM Framework Programme, within the RTD Integrated Project NURESIM "European Platform for Nuclear Reactor Simulations", contract number 516560 (FI6O). The work of the first authors is part of their PhD thesis and has been supported by the *Universidad Politécnica de Madrid* and the *Consejo de Seguridad Nuclear* (Spain).

REFERENCES

1. Chao, Y.A.,"A Theoretical Analysis of the Coarse Mesh Finite Difference Representation in Advanced Nodal Methods", *Mathematics and Computation, Reactor Physics and Environmental Analysis in Nuclear Applications*, J.M. Aragonés (Ed.), **Vol. 1**, 117-126, Senda Ed., Madrid, (1999).
2. Aragonés J.M., Ahnert C., García-Herranz N., "The Analytic Coarse-Mesh Finite-Difference Method for Multigroup and Multidimensional Diffusion Calculations", *Nuc. Sci. & Eng.*, **157**, pp. 1-15 (2007).
3. Lozano, J.A., Aragonés, J.M., García-Herranz, N., "Development and Performance of the Analytic Nodal Diffusion Solver ANDES in Multigroups for 3D Rectangular Geometry", *M&C/SNA-2007*, Am. Nucl. Soc. Monterey, (2007).
4. Lozano, J.A., García-Herranz, N., Ahnert, C., Aragonés, J.M., "The analytic nodal diffusion solver *ANDES* in multigroups for 3D rectangular geometry: development and performance analysis", *Annals of Nuclear Energy*, to be printed in 2008.

5. Jackson J.W., Todreas N.E., “COBRA-IIIc/MIT-2: A Computer Program for Steady State and Transient Thermo-Hydraulic Analysis of Rod Bundle Nuclear Fuel Elements”, MIT report (1981).
6. Lozano J.A., Aragonés J.M., García-Herranz N., “Transient Analysis in the 3D Nodal Kinetics and Thermal-Hydraulics ANDES/COBRA coupled system”, *PHYSOR-2008*, Interlaken, Switzerland, (2008).
7. Jiménez J., Avramova A., Cuervo D., Ivanov K., “Comparative analysis of neutronics /thermal-hydraulics multi-scale coupling for LWR analysis”, *PHYSOR-2008*, Interlaken, Switzerland, (2008).
8. Kolev N.P. et al., “Specifications of the V1000CT2-EXT2 multi-physics Benchmark of NURESIM-SP1, Milestone 20b, Work package T1.4.3”, January (2007).
9. Ivanov B. et al., “VVER-1000 Coolant Transient Benchmark-Phase 1 (V1000CT-1), Volume 1, Final Specifications (Revision 4)”, PennState University, Pennsylvania, USA, 2004
10. Jiménez J., Cuervo D., Aragonés J.M., “Multi-scale and Multi-physics coupling in COBAYA3”, *NURETH-12*, Pittsburgh, USA, (2007).
11. Ivanov B. et al., “VVER-1000 Coolant Transient Benchmark-Phase 1 (V1000CT-1), Volume 3, Summary Results of Exercise 2 on Coupled 3D Kinetics/Core Thermal-hydraulics”, PennState University, Pennsylvania, USA, (2007).